Proceedings of the Korean Nuclear Society Spring Meeting
Cheju, Korea, May 1996

Modeling Heterogeneous Wall Nucleation in Flashing Flow of Initially Subcooled Water

Jong-Woon Park
Institute for Advanced Engineering

Abstract

An analytical model to calculate rate of vapor generation due to heterogeneous wall nucleation in flashing flow is developed. In the present model, an important parameter of the vapor generation term, i.e., nucleation site density is calculated by integrating its probability distribution function with respect to active cavity radius. The limits of integration are minimum and maximum active cavity radii, and these are formulated using an active cavity model for nucleate boiling. This formulation, therefore, can statistically account for the effect of surface specific thermo-physical and geometric conditions on the vapor generation rate and flashing inception. For verifying the adequacy of the present model, steady state two-fluid and the bubble transport equations are solved with applicable constitutive equations. The applicable region of the bubble transport equation is also extended to churn-turbulent flow regime to predict interfacial area concentration at high void fraction. Predicted results in terms of axial pressure and void fraction profiles along the channels are compared with experimental data of Super Moby Dick and BNL. Reasonable agreements have been achieved and this shows the applicability of the present model to flashing flow analysis.

1. Introduction

A subcooled liquid flowing through pipes or nozzles flashes into vapor when its pressure decreases abruptly below saturation pressure by friction and/or acceleration. This principle has been applied in the design of flash cooler, boiler, desalination facility, refrigeration and extensively studied for nuclear reactor safety analysis. Previous typical experiment [1] shows that flashing inception position highly depends not only on the flow but on the wall surface conditions, and the process of vapor generation is certainly dominated by heterogeneous nucleation from the wall similarly to convective boiling where bubbles usually grow from micro-cavities in the wall surfaces. The surface condition can be described by probability distribution functions with parameters such as cavity density, mean cavity radius, mean cone angle, and its standard deviation [2,3]. A numerical model, therefore, should represent this statistical nature of the nucleation process in a flow field.

Previous representative numerical models have been focused on the modeling of bubble nucleation mechanism from the channel wall [4-6]: Dobran [4] used a constant value of bubble density. This is the most simple model. Ardron [5] used expressions derived from kinetic theory for the vapor nuclei production rate as a function of the mass of the molecule and critical work required to create an unstable bubble nucleus. Riznic and Ishii [6] have used a correlation type nucleation model. In case of the last two studies, bubble number density transport equation are solved. These models, however, are unable to express the statistical nature of nucleation process.

The purpose of this paper is to present a new analytical model to calculate vapor generation rate due to heterogeneous wall nucleation in flashing flow using probability distribution function of nucleation sites. Active nucleation site density is calculated as a function of minimum and maximum cavity radii. The minimum active cavity radius is theoretically derived by applying nucleation theory developed in the previous studies on the nucleate boiling. Separate conservation equations for the two phases are used to validate present model against the experimental data.

2. Mathematical Model

2.1 Two-Fluid Model

The non-equilibrium two-phase flow can be best estimated using the six-equation two-fluid model. The steady state conservation equations of mass, momentum, and energy described by Bestin [7] are

given by

$$\frac{1}{A}\frac{d}{dz}A\alpha_k\rho_k V_k = \Gamma_k \tag{1a}$$

$$\frac{1}{A}\frac{d}{dz}\alpha_k\rho_k V_k^2 + \alpha_k\frac{dp}{dz} = -\frac{P_e}{A}\tau_{wk} - \tau_{ik} - \tau_{vmk} - p_i\frac{d\alpha_k}{dz} + \Gamma_k V_{ik} + \alpha_k\rho_k g \tag{1b}$$

$$\frac{1}{A}\frac{d}{dz}A\alpha_k\rho_k V_k\left(h_k + \frac{V_k^2}{2}\right) = q_{ki} + \Gamma_k\left(h_k + \frac{1}{2}V_k^2\right) + \alpha_k\rho_k V_k g \tag{1c}$$

where symbols have their usual meanings in two-phase flow and k stands for liquid or vapor phase. Also note the following interfacial jump conditions: $\sum_{k=l,g}\Gamma_k = 0$; $\sum_{k=l,g}\tau_{ik} = 0$; and $\sum_{k=l,g}\tau_{vmk} = 0$.

The vapor generation rate Γ in Eqs.(1a) and (1c) consists of Γ_g, the convective mass transfer due to difference in temperatures of two phases and Γ_n, the vapor generation due to heterogeneous wall nucleation. The major portion of this paper is contributed to the description of a new analytical model for Γ_n. Well known constitutive equations, listed in Table 1 are selected for other parameters.

2.2 Flash Vapor Generation Rate due to Heterogeneous Wall Nucleation

The vapor generation rate resulting from the heterogeneous wall nucleation can be expressed as

$$\Gamma_n = \frac{4}{D}N_{ns}f_d V_d \rho_g \tag{2}$$

where D is the channel diameter, N_{ns} is the nucleation site density, f_d and V_d are the departure frequency and the volume of departing bubble.

N_{ns} in Eq.(2) is dependent on the surface characteristics with major parameters of cavity radius r_c and half cone angle of the cavity β who have gamma and normal distributions, respectively [3]:

$$f(r_c) = \frac{1}{r_{c,m}}\exp\left(-\frac{r_c}{r_{c,m}}\right) \tag{3}$$

$$g(\beta) = \frac{1}{(2\pi)^{1/2}s}\exp\left(-\frac{(\beta - \beta_m)^2}{2s^2}\right) \tag{4}$$

where s is the standard deviation of β and subscript m denotes the mean value. Therefore, N_{ns} can be calculated from the integral of the two functions applying integral limits such that $\beta < \theta/2$ for β from entrapment condition [8] where θ is the contact angle, and $r_{c,min}$ and $r_{c,max}$, for r_c:

$$N_{ns} = N_m\int_0^{\theta/2} g(\beta)d\beta \int_{r_{cmin}}^{r_{cmax}} f(r_c)dr_c \tag{5}$$

where N_m is the average number density of cavities on the surface. Since the angle θ in Eq.(5) is already known, the integral with respect to β can be performed first of all.

When the bubbles are nucleating from the wall, although bulk liquid core may be superheated, local average wall temperature is between the superheated bulk liquid and local saturation temperatures, and therefore radial flow field can be divided into the turbulent liquid core region with uniform superheated temperature and near-wall thermal boundary layer (TBL) with thickness δ_t as shown in Fig. 1 [9].

Given the saturation temperature at system pressure T_{sat}, bubble temperature T_b is obtained as a function of the bubble nucleus height y_b [10] (see Fig.1):

$$T_b(y_b) = T_{sat} + \frac{2\sigma T_{sat}}{\rho_g h_{lg}}\frac{1+\cos\phi}{y_b} \tag{6}$$

where σ is the Stefan-Boltzmann constant and h_{fg} is the latent heat of vaporization

Assuming a linear temperature profile in the TBL, we get

$$T_l(y) = T_w + \frac{T_{lm} - T_w}{\delta_t}y \tag{7}$$

where T_{lm} and T_w are the temperatures of the liquid core and the wall, respectively, and δ_t is the effective TBL thickness given by

$$\delta_t = \frac{D}{\mathrm{Nu}_{l,D}} \tag{8}$$

where $Nu_{l,D}$ is the Nusselt number of forced convective cooling.

The two equations (6) and (7) are plotted in Fig.1. Below the crossed point, liquid temperature is still lower than the required temperature for nucleation, and therefore a bubbles with height less than y_b (corresponding to cavity radius r_c) cannot absorb enough thermal energy to grow. This limiting cavity radius is referred to as a minimum effective (candidate to grow) cavity radius $r_{c,min}$ and obtained by equating Eq.(6) to Eq.(7) and using the relationship between y_b and r_c [10].

$$r_{c,\min} = \frac{\delta_t}{2}\left\{ \frac{T_{sat}-T_w}{T_{lm}-T_w} + \left[\left(\frac{T_{sat}-T_w}{T_{lm}-T_w} \right)^2 + \frac{2\sigma T_{sat}}{\rho_g h_{lg}} \frac{1+\cos\phi}{\delta_t (T_{lm}-T_w)} \right]^{1/2} \right\} \tag{9}$$

As for the maximum effective cavity radius, $r_{c,max}$ in Eq.(5), a bubble with height greater than the TBL thickness cannot meet with more superheated liquid for further growth to the departure size [9], therefore it is assumed that

$$r_{c,\max} = \frac{\sin\beta}{1+\cos\beta}\ \delta_t \tag{10}$$

where β is the cone angle of the cavity.

Therefore, a necessary condition for a bubble to be effective is that the liquid temperature profile should be the form designated by (b) rather than (a) as shown in Fig. 1. All the cavities within the effective range ($r_{c,min} < r_c < r_{c,max}$) are assumed to be active (able to grow) ones.

The accurate estimation of the wall temperature T_w in Eq.(9) is very complex and beyond the scope of this paper, and thus in this paper wall temperature is calculated from simple steady state conjugate heat balance through radial direction.

2.3 Transport Equation of Bubbles

The one-dimensional steady state transport equation of small bubbles in bubbly and churn-turbulent flow regimes is [8]

$$N\frac{dV_g}{dz} + V_g\frac{dN}{dz} = -\frac{V_g N}{A}\frac{dA}{dz} + \dot{N}_n - \dot{N}_c \tag{11}$$

where N is the bubble number density (number per unit volume of two-phase mixture), $\dot{N}_n$ and $\dot{N}_c$ are the production and annihilation rates of small bubbles, respectively.

The bubble nucleation rate $\dot{N}_n$ in Eq.(11) can be obtained from

$$\dot{N}_n = \frac{4}{D} N_n f_d \tag{12}$$

where f_d is the bubble departure frequency given by Zuber [11], and the implicit departure diameter d_d is calculated from the correlation of Kocamusfataogulari and Ishii [12].

The bubble annihilation rate $\dot{N}_c$ in Eq.(11) is important in a bubbly-to-churn turbulent flow regime transition. From the fact that the rate of decrease of small bubble void fraction is the same as the rate of increase of Taylor bubble void fraction, and assuming linear variation of void fraction from bubbly to churn-turbulent flow regime [1] $\dot{N}_c$ is given by

$$\dot{N}_c = \frac{V_g}{v_b} u(\alpha_b, \alpha_a) \frac{1}{1-\alpha_b}\left[1 + \alpha_b \frac{(1-\alpha_b)}{(\alpha_a-\alpha_b)} \right] \frac{d\alpha}{dz} \tag{13}$$

where α_t is the void fraction contributed from Taylor bubbles and v_b is the volume of a small bubble, $u(\alpha_b, \alpha_b)$ is the step function whose value is 1 if $\alpha_b < \alpha < \alpha_a$ and 0 elsewhere.

3. Results and Discussion

For the liquid before flashing, single-phase equations for the liquid velocity, pressure and temperature are obtained by using fifth-order Runge-Kutta predictor corrector method. For the two-phase region downstream of the flashing inception location, the two-phase conservation equations (1a)-(1c), and the bubble number density transport equation Eq.(11) are rearranged to obtain a system of first order ordinary differential equations with dependent variables of velocities and enthalpies of liquid and vapor, pressure, void friction and bubble number density. This system of equations are also solved by means of fifth-order Runge-Kutta predictor corrector method.

To investigate the prediction capability of the present model, existing experimental data obtained from the condition where one dimensional flow is dominating are selected from the literatures. The flashing flow experiments carried out by Abauf et al. (BNL) [1] and Rousseau (Super Moby Dick) [13] highlights the interphase mass, momentum, and heat transfers with accompanying data of pressure and/or void fraction profiles along the channels under a large variety of high pressure conditions (from 0.1 up to 12MPa). In this paper, thus the model predictions are compared with some of these experimental data.

In the case of the experimental data of Super Moby Dick [13], the pressure and void fraction profiles along the axial direction are available to the author for only the Run #40B240C. Test section geometry is also shown in Fig.2. The inlet pressure and temperature are 4.002 MPa and 240.5 °C, respectively, for which the inlet subcooling is 9.87 °C. For the model prediction, the same inlet condition are used, and $N_m = 2.3 \times 10^7$ are assumed for the calculation of nucleation site density in Eq.(5). It is shown in Fig. 2 that the pressure profile is predicted very accurately by present model. The void fraction data is somewhat larger in the constant pipe section and somewhat smaller in the diffuser section near the throat. This is due to the fact that in the experiment the situation is critical whereas calculation cannot proceed beyond the critical point and the profiles obtained by the prediction are under subcritical condition. This makes the predicted pressure gradient at the throat smaller than in the experiment, so that the predicted evaporation rate is smaller and this is further reflected in the smaller void fraction in the diffuser section near the throat. The critical mass flux in the experiment is 32800 kg/m^2-sec and the assumed mass flux at the throat is 32897 kg/m^2-sec. The two values are very close to each other.

A typical experimental run #309 of BNL [1] is compared with predicted results. Figure 3 shows the nozzle used in the experiment. The inlet pressure and temperature of the run is 0.556 MPa and 149.1 °C, respectively where inlet subcooling is 6.78°C. For the prediction of the axial pressure and void fraction profiles by the present model, the same inlet condition is used. Assumed value of N_m is 3.4×10^6. The critical mass flux measured in the experiment is 4330 kg/m^2-sec and the same value is assumed in the prediction. It can be shown from Fig.3 that the pressure and void fraction profiles are predicted very accurately by the present model. Figure 4 shows the calculated parameters such as T_l, T_g, V_l, V_g, Γ_g, Γ_n, N, and a in this case. It can be known from Fig.4 that the liquid and vapor temperatures are nearly the same as initial liquid temperature and saturation temperature at the local pressure, respectively. The vapor generation due to wall nucleation Γ_n is dominant mass transfer mechanism in the flashing inception region, however, further downstream of the nozzle throat it becomes comparable to the vapor generation of existing bubble Γ_g. The bubble number density N and interfacial area a concentration sharply decrease when the void fraction is greater than 0.3 due to bubble coalescence in bubbly-to-churn turbulent flow regime transition. The volume averaged velocities of each phases increase from the flashing inception region to the nozzle throat, and in the diverging region the liquid is more decelerates due to its mass but the vapor is still accelerating since the liquid is still evaporating.

4. Conclusion

An analytical model for the vapor generation rate from heterogeneous wall nucleation in flashing flow is developed, and its adequacy is tested by applying into the two-fluid model. The results are compared with existing experiments such as Super Moby Dick and BNL. The agreements were satisfactory and this shows the present statistical model of nucleation process is reasonable approach in the calculation of flash evaporation rate.

References

1. Abauf, N. and Zimmer, G.A., and Wu, B.J.C., "A Study of Nonequilibrium Flashing of Water in a Converging Diverging Nozzle," NUREG/CR-1864, BNL-NUREG- 51317, Vol.1: Experimental and Vol.2: Theoretical, 1981.
2. Nail, J.P., Jr., Vachon, R.I., and Morehouse, J., "An SEM Study of Nucleation Sites in Pool

Boiling from 304 Stainless Steel," Trans. ASME J. Heat Transfer, May, pp.132-137, 1974.
3. Yang, S.R. and Kim, R.H., "A Mathematical Model of the Pool Boiling Nucleation Site Density in Terms of the Surface Characteristics, Int. J. Heat Mass Transfer, Vol.31, No. 6, pp.1127-1135, 1988.
4. Dobran, F., "Nonequilibrium Modeling of Two-Phase Critical Flows in Tubes," Trans. ASME J. Heat Transfer, Vol. 109, pp.731-738, 1987.
5. Ardron, K.H., "A Two-Fluid Model for Critical Vapor-Liquid Flow," Int. J. Multiphase Flow, Vol. 4, No. 3, pp.323-337, 1978.
6. Riznic, J. and Ishii, M., "Bubble Number Density and Vapor Generation in Flashing Flows," Int. J. Heat Mass Transfer, Vol. 32, pp.1821-1833, 1989.
7. Bestin, D., "The Physical Closure Laws in the CATHARE code," Nuclear Engineering and Design, Vol. 124, pp.229-244, 1990.
8. Bankoff, S.G., "Entrapment of Gas in the Spreading of a Liquid over a Rough Surface," AIChE J., Vol. 4, pp.24-26, 1958.
9 Peterson, P.F. and Hijikata, K., "Conjugate Heat Transfer Effects on Wall Bubble Nucleation in Subcooled Flashing Flows, "In Advances in Gas-Liquid Flows presented at the Winter Annual Mtg. of the ASME, Dallas, Texas, Nov. 25-30, 1990.
10. Hsu, Y.Y., "On the Size Range of Active Nucleation Cavities on a Heating Surface," Trans. ASME. J. Heat Transfer, Vol. 94, August, pp.207-216, 1962.
11. Zuber, N., "Nucleate Boiling : The Region of Isolated Bubbles and the Similarity with natural convection," Int. J. Heat Mass Transfer, Vol. 6, pp.53-78, 1963.
12. Kocamusfataogulari, G. and Ishii, M., "Interfacial Area and Nucleation Site Density in Boiling System," Int. J. Heat Mass Transfer, Vol. 26, pp.1377-1387, 1983.
13. Rousseau, J.C.," Flashing Flow," Multiphase Science and Technology (edited by Hewitt, G.F., Delhaye, J.M., and Zuber, N., Vol.3, pp.378-389, 1987.

Table 1. Constitutive equations in the conservation equations

Constitutive Equations
Convective Mass Transfer: $\Gamma_g = \frac{h\,(T_l - T_g)}{h_g - h_l}$
B: $h = \frac{k_l}{d_b}(2 + 0.6Re_b^{1/2}\mathrm{Pr}_l^{1/3})$; C: $h = (h_{sb}\,a_{sb} + h_{tb}\,a_{tb})$ where $h_{tb} = 0.0073\,\rho_l V_l c_{pl}$; A: $h = \frac{k_g}{D\alpha^{1/2}} = 0.023Re_{g\alpha}^{0.8}\mathrm{Pr}_g^{0.4}$
Interfacial Shear Stress: $\tau_i = \frac{1}{8}a_i C_D \rho_g \frac{\lvert V_r\rvert V_r}{2}$
B: $C_D = \frac{24}{Re_b}(1+0.1Re_b^{0.75})$; C: $C_D = \frac{3}{8}(1-\alpha)^2$; A: $C_D = 0.079Re_g^{-0.25}\left[1+24(1-\alpha^{1/2})(\frac{\rho_l}{\rho_g})^{1/3}\right]$
Wall Shear Stress: $\tau_{wl} = \phi^2\frac{4}{D}f_{lo}\frac{G^2}{2\rho_l}$; ϕ^2 : two-phase frictional multiplier; f_{lo} : single-phase friction factor of the liquid phase
Virtual Mass Force: $\tau_{vm} = C_{vm}\alpha(1-\alpha)\,[\alpha\rho_g+(1-\alpha)\rho_l]\left(V_g\frac{dV_g}{dz} - V_l\frac{dV_l}{dz}\right)$; $C_{vm} = 0.5\frac{1+2\alpha}{1-\alpha}$ for $\alpha \le 0.5$; $C_{vm} = 0.5\frac{3-2\alpha}{\alpha}$ for $\alpha > 0.5$
Interfacial Area Concentration: B: $a = (N\pi)(6\alpha)^{2/3}$; C: $a = a_{sb} + a_{tb}$ where $a_{sb} = (N\pi)(6\alpha_{sb})^{2/3}$; $a_{tb} = \frac{4\alpha_{tb}^{2/3}}{\alpha_a^{1/6}D}$; $\alpha_{sb} = \alpha - \alpha_{tb}$; $\alpha_{tb} = \frac{1}{1-\alpha_b}\left[\alpha - \alpha_b(1 - \frac{(1-\alpha_a)(\alpha-\alpha_b)}{(\alpha_a-\alpha_b)})\right]$ A: $a = \frac{4}{D}\alpha^{1/2}$
Interfacial Pressure: $p_i = \frac{\alpha(1-\alpha)\rho_g\rho_l}{\alpha\rho_g + (1-\alpha)\rho_l}V_r^2$: non stratified flow
Relative Velocity: $V_r = \frac{(1-C_o\alpha)}{1-\alpha}V_g - C_oV_l$ where $C_o = C_\infty - (C_\infty - 1)\left(\frac{\rho_l}{\rho_g}\right)^{1/2}$; $C_\infty = 1+0.2\left[\frac{\rho_l\sqrt{gD}}{G}\right]^{1/2}$
Reynolds Numbers: $Re_b = \frac{(1-\alpha)d_b\rho_l\lvert V_r\rvert}{\mu_l}$; $Re_g = \frac{\rho_g D\lvert V_r\rvert}{\mu_g}$; $Re_{g\alpha} = \frac{\rho_g D\alpha^{1/2}\lvert V_r\rvert}{\mu_g}$

(Note) B: bubbly flow; C: churn-turbulent flow; A: annular flow; subscript *sb*: between small bubbles and liquid phase; subscript *tb* : between large Taylor bubbles and liquid phase

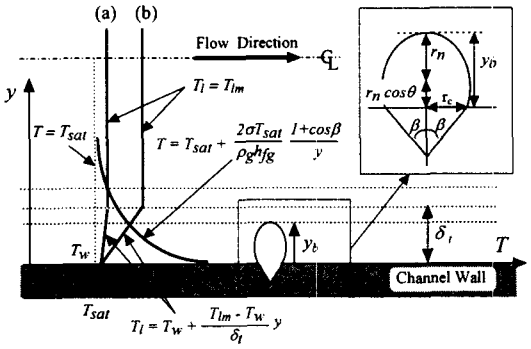

Fig.1 Schematic of superheated liquid temperature profiles near the channel wall and a bubble growing from the wall cavity in flashing flow

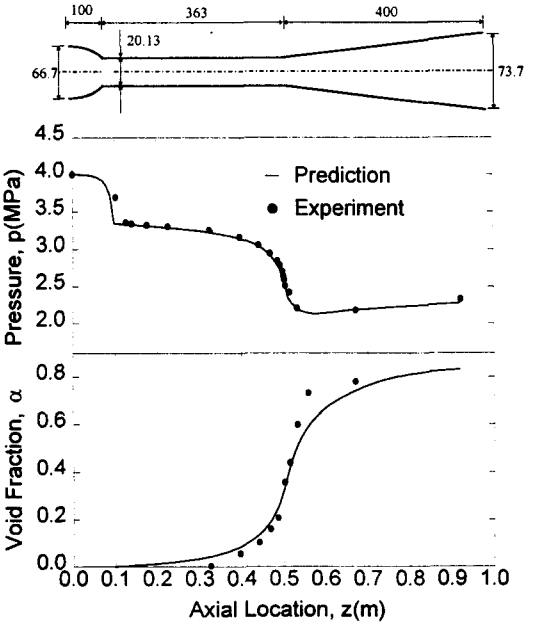

Fig.2 Predicted and experimental pressure and void fraction profiles (Super Moby Dick RUN #40B240C: P_o = 4.002 MPa, T_o = 240.5°C, ΔT_{sub} = 9.87°C, G_{exp} = 32800 kg/m^2-sec, $G_{predict}$ = 32897 kg/m^2-sec)

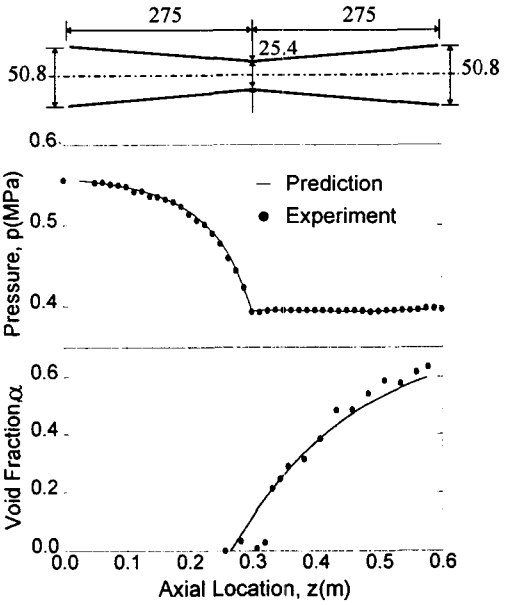

Fig.3 Predicted and experimental pressure and void fraction profiles (BNL RUN #309: P_o = 0.556 MPa, T_o = 149.1°C, ΔT_{sub} = 6.78°C, G_{exp} = 4330 kg/m^2-sec, $G_{predict}$ = 4330 kg/m^2-sec)

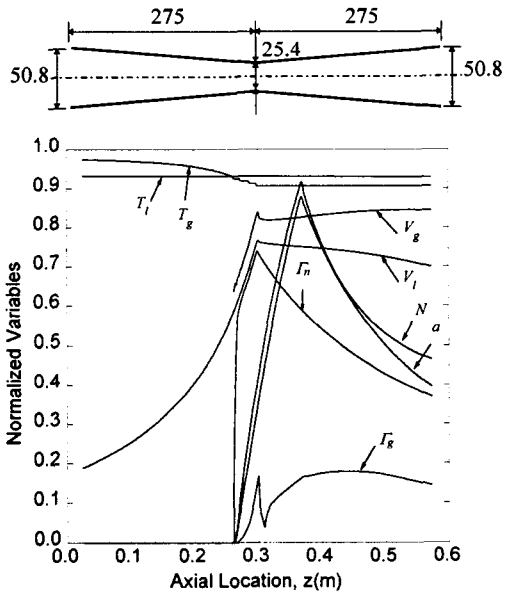

Fig.4 Calculated parameters along the BNL nozzle (RUN #309: P_o = 0.556 MPa, T_o = 149.1°C, ΔT_{sub} = 6.78°C, G_{exp} = 4330 kg/m^2-sec, $G_{predict}$ = 4330 kg/m^2-sec)